

# SPIN-CROSSOVER IN MOLECULAR CRYSTALS: AN ELECTRON-COUPLED LOCAL VIBRATIONS MODEL

## TRANSICIÓN DE ESPÍN EN CRISTALES MOLECULARES: UN MODELO DE ELECTRONES Y VIBRACIONES LOCALES ACOPLADAS

C. RODRÍGUEZ-CASTELLANOS<sup>a,b,†</sup>, Y. PLASENCIA<sup>a</sup>, E. REGUERA<sup>a</sup>

a) Centro de Investigación en Ciencia Aplicada y Tecnología Avanzada (CICATA-Legaria), Instituto Politécnico Nacional, 11500 Ciudad de México, México

b) Facultad de Física, Universidad de La Habana, 10400 La Habana, Cuba; crc@fisica.uh.cu<sup>†</sup>

<sup>†</sup> corresponding author

Recibido 21/5/2018; Aceptado 21/9/2018

A model of eg electrons at octahedral sites coupled to local vibrational “breathing” modes interacting with its near neighbors is proposed to describe spin-crossover (SCO) in molecular crystals. Decoupling vibrations leads to an effective electron Hamiltonian with renormalized site energies, where ferromagnetic and antiferromagnetic, short range and long range electron-electron interactions arise in a natural way. An exact analytic expression for the free energy functional is derived. A phase diagram for homogenous phases, describing the basic phenomenology of SCO is obtained and the transition temperatures are expressed in terms of model parameters. Under appropriate conditions, two-step transitions are found to take place for systems with both, short range and long range interactions. Stability with respect to spatial fluctuations is discussed.

Para describir la transición de espín (SCO) en cristales moleculares se propone un modelo de electrones eg acoplados a modos de vibración locales “respiratorios” que interactúan con sus vecinos próximos. Al desacoplar las vibraciones resulta un Hamiltoniano electrónico efectivo con energías renormalizadas, donde las interacciones electrón-electrón ferromagnéticas y anti-ferromagnéticas, de corto y de largo alcance aparecen de modo natural. Se deriva una expresión analítica exacta para el funcional de energía libre. Se obtiene un diagrama de fases homogéneas que describe la fenomenología básica de la transición de espín y se calculan las temperaturas de transición en función de los parámetros del modelo. Bajo condiciones apropiadas, las transiciones en dos pasos resultan posibles tanto en sistemas con interacciones de corto como de largo alcance. Se discute la estabilidad respecto a las fluctuaciones espaciales.

PACS: Statistical mechanics of model systems (Mecánica estadística de sistemas modelo), 64.60 De; Spin crossover (Cruce de spin), 75.30. Wx; Molecular magnetism (Magnetismo molecular), 75.50. Xx

### I. INTRODUCTION

Spin-crossover (SCO) is the transition between a low spin (LS) and a high spin (HS) state of a metal ion with  $d^4$ - $d^7$  electronic configuration in an octahedral ligand field, under the action of external stimuli. The phenomenon has a wide presence in nature, especially in the case of the transition of  $\text{Fe}^{\text{II}}$  complexes between  $t_{2g}^6$  ( $S=0$ ) and  $t_{2g}^4 e_g^2$  ( $S=2$ ) configurations, which is responsible for oxygen transport in hemoglobin and probably for the change under pressure of ferroperricite in the Earth's mantle. In solids, SCO can be found in many transition metal oxides, organometallic complexes, inorganic salts or organic radicals and has a cooperative nature, frequently leading to abrupt changes of macroscopic physical properties and hysteresis. A clear introduction and a broad perspective of the field can be found in the monographs [1] and [2].

The most common way of monitoring spin transitions is a plot of the HS fraction versus temperature, conventionally obtained from magnetic measurements or Mössbauer spectroscopy [3]. These spin transitions curves can be gradual, abrupt, hysteretic, two-steps or incomplete, depending on the degree of cooperativity of the spin system [4]. Complementary information about changes in structure and physical properties during the spin transition is obtained with the aid of many other experimental techniques.

Materials with abrupt SCO near room temperature and wide hysteresis loops are the focus of research in the field, because of potential applications in molecular electronics and spintronics [5]. The big theoretical challenge is to predict the spin transition curve for a specific material, including the transition temperatures and the width of the hysteresis loops. Macroscopic and semi-microscopic approaches, based in Landau theory of phase transitions and Ising-like models have contributed to the progressive understanding of SCO and related phenomena [6, 7]. A complete microscopic description requires the consideration of three basic elements: i) the spin and vibrational states of individual octahedral complexes, ii) the interactions between them leading to cooperative effects and iii) their connection to external factors like temperature, hydrostatic pressure, light irradiation, magnetic field and the chemical environment. Given the diverse nature of SCO compounds, it is unlikely that a single theory could account for all different behaviors. For example, in oxides cooperativity is attributed to electronic exchange and in molecular crystals to electron-phonon coupling [8]. Recent contributions [9] emphasize the key importance of strong coupling between eg electrons and molecular fully symmetric (“breathing”) vibration modes (instead of Jahn-Teller vibrations as previously proposed [10,11]) in determining the local energy pattern of SCO in molecular crystals. On the other hand, the

responsibility for cooperative phase transitions is attributed to the interaction with acoustic phonons propagating along the crystal. This difference had already been considered in phenomenological approaches through the introduction of two different elastic constants [12]. In reference [9] a detailed Hamiltonian containing the interactions between electrons, acoustic phonons and local fully symmetric vibrations has been proposed. After explicit shift transformation of phonon operators they are decoupled, leading to an effective, phonon mediated, electron-electron interaction, additional to the quadratic interaction with local vibrational modes. The approach has been generalized to SCO in binuclear compounds [13]. Unfortunately, such a detailed description requires drastic approximations (mean field, simple phonon models) to evaluate the HS fraction as a function of temperature. This paper presents a theoretical approach to SCO in mononuclear molecular crystals containing Fe<sup>II</sup> ions, based in the same idea of reference [9], but in a simplified version. Instead of coupling to acoustic phonons, a simple effective interaction between neighboring local breathing modes is considered. Only electrons in e<sub>g</sub> states are linearly coupled to vibrations, so there is no need for two breathing modes with different vibrational frequencies and coupling parameters. Next, decoupling breathing modes with successive canonical transformations leads to a lattice model where short range and long range ferromagnetic and antiferromagnetic interactions arise in a natural way. A general discussion of the phase diagram predicted by this model is possible without appeal to additional approximations.

## II. MODEL

Consider a d-dimensional periodic array of ( $i = 1, \dots, N$ ) mono-nuclear metal complexes, each containing an ion Fe<sup>II</sup> in an octahedral site surrounded by non-magnetic ligands. The number of electrons occupying e<sub>g</sub> states at ion “ $i$ ” will be designed by  $n_i$ . Since the charge density distribution of the anti-bonding e<sub>g</sub> states is more localized near their octahedral neighbors, these electrons, and not those at states t<sub>2g</sub>, are strongly coupled to a local “breathing” vibration mode described by operators  $\hat{a}_i^+$ ,  $\hat{a}_i$ . Breathing modes at neighboring sites interact through acoustic phonons. The effective Hamiltonian for this electron-local vibrations system will be:

$$\hat{H} = \sum_{i=1}^N \hat{H}_i + \sum_{\langle i,j \rangle} \hat{V}_{ij}, \quad (1)$$

$$\hat{H}_i = \varepsilon n_i + \left( \hat{a}_i^+ \hat{a}_i + \frac{1}{2} \right) - \alpha n_i (\hat{a}_i^+ + \hat{a}_i), \quad (2)$$

$$\hat{V}_{ij} = -\frac{\lambda}{4} (\hat{a}_i^+ + \hat{a}_i) (\hat{a}_j^+ + \hat{a}_j). \quad (3)$$

In these expressions  $\varepsilon > 0$  is the excitation energy per e<sub>g</sub> electron, obtained by subtracting the splitting energy  $\Delta$  between t<sub>2g</sub> and e<sub>g</sub> states and the pairing energy  $P$  in t<sub>2g</sub> states, while  $\alpha$ ,  $\gamma$  are coupling parameters. The phonon energy  $\hbar\omega$  of the local breathing mode when the ion is in

the HS state has been taken equal to one. This energy, in the order of 10<sup>2</sup> cm<sup>-1</sup>, is too low to produce real transitions between different electron states ( $\varepsilon \sim 10^3$  cm<sup>-1</sup>). Coupling to local modes induces virtual transitions that renormalize electron energies, give rise to an effective electron-electron interaction and shift atomic positions (see below). To clarify the assumptions usually involved in this kind of model and to give the possibility to go beyond them, a detailed derivation has been included in the Supplementary Information [SA] accompanying this paper. The interaction Hamiltonian  $\hat{V}_{ij}$  is the simplest approximation to an effective inter-site coupling which could result from averaging over degrees of freedom (acoustical phonons) connecting local breathing modes at neighboring sites [9].

Breathing modes can be decoupled by canonical transformations of their creation and annihilation operators, leading to a system with an effective electron-electron interaction and independent dispersive phonons [SB]:

$$\hat{H} = \hat{H}_e + \hat{H}_{ph}, \quad (4)$$

$$\hat{H}_e = \sum_{i=1}^N (\varepsilon n_i - \alpha^2 n_i^2) - \alpha^2 \lambda \sum_{\langle i,j \rangle} n_i n_j - \sum_{i,j} U_{ij} n_i n_j, \quad (5)$$

$$\hat{H}_{ph} = \sum_{\vec{q}} \sqrt{|1 - \lambda s(\vec{q})|} \left( \hat{a}_{\vec{q}}^+ \hat{a}_{\vec{q}} + \frac{1}{2} \right) \quad (6)$$

$$U_{ij} = \frac{\alpha^2 \lambda^2}{N} \sum_{\vec{q}} \frac{s^2(\vec{q})}{1 - \lambda s(\vec{q})} e^{i\vec{q} \cdot (\vec{R}_i - \vec{R}_j)}, \quad (7)$$

$$s(\vec{q}) = \frac{1}{2} \sum_{j(i)=1}^z e^{i\vec{q} \cdot (\vec{R}_i - \vec{R}_j)}. \quad (8)$$

In the above summations, symbols  $j(i)$  and  $\langle i, j \rangle$  denote near-neighboring sites  $j$  for fixed  $i$  and pairs of neighbors respectively. The electron configuration is defined by  $\{n_i\}$ . The wave vector  $\vec{q}$  takes  $N$  values in the first Brillouin zone of the periodic structure formed by the Fe<sup>II</sup> ions at the octahedral sites. Inversion symmetry has been assumed, so that  $s(\vec{q}) = s(-\vec{q})$ .

For weak inter-site coupling ( $\lambda z < 2$ ) the quantity  $1 - \lambda s(\vec{q})$  is positive and no soft modes are generated by the interaction. The average shift in equilibrium atomic positions due to a change in spin –state is proportional to [SA]:

$$\frac{\langle \hat{a}_i + \hat{a}_i^+ \rangle}{2} = \alpha \langle n_i \rangle + \frac{\alpha \lambda}{N} \sum_j \langle n_j \rangle \sum_{\vec{q}} \frac{s(\vec{q})}{1 - \lambda s(\vec{q})} e^{i\vec{q} \cdot (\vec{R}_i - \vec{R}_j)}.$$

According to 5, the renormalized energy  $\varepsilon^*$  of e<sub>g</sub> electron states and the effective in-site interaction  $u^*$  between them are given by:

$$\varepsilon^* = \varepsilon - \alpha^2 - \frac{\alpha^2 \lambda^2}{N} \sum_{\vec{q}} \frac{s^2(\vec{q})}{1 - \lambda s(\vec{q})} e^{i\vec{q} \cdot (\vec{R}_i - \vec{R}_j)},$$

$$u^* = -\alpha^2 - \frac{\alpha^2 \lambda^2}{N} \sum_{\vec{q}} \frac{s^2(\vec{q})}{1 - \lambda s(\vec{q})} e^{i\vec{q} \cdot (\vec{R}_i - \vec{R}_j)}.$$

Coupling to phonon modes lowers the energy of one electron states ( $\varepsilon^* < \varepsilon$ ) and leads to attractive in-site interaction between them ( $u^* < 0$ ) at least for weak inter-site coupling ( $\lambda z < 2$ ). This favors local high spin states at finite temperatures. The interaction  $-\alpha^2 \lambda$  between  $e_g$  electrons at neighboring sites is also attractive and leads to the collectivization of HS states.

On the other hand, the effective interaction  $U_{ij}$  between  $e_g$  electrons at arbitrary different sites is also attractive and short ranged for  $\lambda z < 2$ , oscillating and long ranged for intermediate coupling ( $2 < \lambda z < 4$ ) and repulsive but short ranged in the strong coupling case ( $\lambda z > 4$ ). For a cubic array with lattice parameter equal to one, in the long distance limit ( $q \rightarrow 0$ ) one has:

$$U_{ij} = \frac{\alpha^2 \lambda^2 z^3}{4 - \lambda z} \frac{1}{N} \sum_{\vec{q}} \frac{e^{i\vec{q}(\vec{R}_i - \vec{R}_j)}}{q^2 + \kappa^2} \sim \frac{1}{4 - \lambda z} \frac{e^{-\kappa R_{ij}}}{R_{ij}},$$

$$\kappa^2 = \frac{2(2 - \lambda z)}{4 - \lambda z}.$$

The statistical sum for the electron system is:

$$Z = \sum_{\{n_i\}} \exp \left\{ -\frac{H_e\{n_i\}}{KT} \right\} \prod_{i=1}^N g_{n_i}. \quad (9)$$

To incorporate into the Hamiltonian the degeneracy  $g_{n_i}$  of local states with  $n_i$  electrons  $e_g$  at site  $i$ , a procedure introduced in [14] for  $n_i = 0, 1$  has been generalized to the case  $n_i = 0, 1, 2$  [SC]:

$$H_e^*\{n_i\} = H_e\{n_i\} - kT \sum_{i=1}^N g_{n_i},$$

$$\sum_{i=1}^N \ln g_{n_i} = N \ln g_0 + \frac{1}{2} \ln \left( \frac{g_1^4}{g_0^3 g_2} \right) \sum_{i=1}^N n_i - \frac{1}{2} \ln \left( \frac{g_1^2}{g_2 g_0} \right) \sum_{i=1}^N n_i^2. \quad (10)$$

To explore the phase diagram let's introduce a free energy functional

$$\varphi[\{n_i\}, T] = \frac{H_e^*\{n_i\}}{N}.$$

In the thermodynamic limit, the minimum of  $\varphi[\{n_i\}, T]$  is the exact free energy per site:

$$f(T) \equiv - \lim_{N \rightarrow \infty} \frac{kT}{N} \ln \sum_{\{n_i\}} \exp \left\{ -\frac{H_e\{n_i\}}{KT} \right\} = \lim_{N \rightarrow \infty} \min \varphi[\{n_i\}, T]$$

The free energy functional can be also expressed in terms of the Fourier components:

$$n_i = \sum_{\vec{q}} \tilde{n}(\vec{q}) e^{i\vec{q} \cdot \vec{R}_i}; \quad \tilde{n}(\vec{q}) = \frac{1}{N} \sum_i n_i(\vec{q}) e^{i\vec{q} \cdot \vec{R}_i}.$$

Then, up to an additive constant:

$$\varphi[\{\tilde{n}(\vec{q})\}, T] = \varepsilon_1 n - \varepsilon_2 n^2 - \sum_{\vec{q} \neq 0} \varepsilon_2(\vec{q}) |\tilde{n}(\vec{q})|^2, \quad (11)$$

$$\varepsilon_1 = \varepsilon - \frac{kT}{2} \ln \left( \frac{g_1^4}{g_0^3 g_2} \right),$$

$$\varepsilon_2(\vec{q}) = \frac{\alpha^2}{1 - \lambda s(\vec{q})} - \frac{kT}{2} \ln \left( \frac{g_1^2}{g_2 g_0} \right),$$

$$n = \tilde{n}(0); \quad \varepsilon_2 = \varepsilon_2(0). \quad (12)$$

The first two terms of 11 give the free energy of a homogenous phase with average spin  $n$  and the last one is the contribution of spatial fluctuations.

### III. PHASE DIAGRAM

For homogenous phases  $n_i = n(0, 1, 2)$ , and the free energy functional 11 reduces to:

$$\varphi[\{n_i = n\}, T] = \varepsilon_n = \varepsilon_1 n - \varepsilon_2 n^2. \quad (13)$$

The phase diagram is shown in figure 1. Low (LS), intermediate (IS) and high spin (HS) phases correspond to regions in the plane  $\varepsilon_2 - \varepsilon_1$  where the absolute minimum of  $\varphi_n$  is obtained for  $n = 0, 1, 2$  respectively. A point on the equilibrium lines correspond to a sequence of states where two phases coexist. The triple point can be reached only under the conditions  $\varepsilon_1 = \varepsilon_2 = 0$ .

At  $T = 0$  K only LS and HS phases can exist. The ground state is in the first (third) quadrant for  $\lambda z < 2$  ( $\lambda z > 2$ ), corresponding to a LS phase when  $\varepsilon > (4\alpha^2)/(2 - \lambda z)$  and to a HS phase in the opposite case. As  $T$  increases at constant pressure, parameters  $\varepsilon_1$  and  $\varepsilon_2$  decrease along the isobars:

$$\varepsilon_1 = \varepsilon + \frac{4 \ln g_1 - 3 \ln g_0 - \ln g_2}{2 \ln g_1 - \ln g_0 - \ln g_2} \left( \varepsilon_2 - \frac{2\alpha^2}{2 - \lambda z} \right). \quad (14)$$

The slope of these straight lines depends only of the degeneracies of local states. Temperature induced first order transitions take place when the isobars 1 cross the phase equilibrium lines, as indicated in figure 1 for  $g_0 = 1$ ;  $g_1 = 9$ ;  $g_2 = 15$ .

When the ground state is HS (isobar-a in the phase diagram), there are no temperature induced phase transitions. For the LS ground state in the first quadrant, both one-step (isobar-b)) and two-step transitions (isobar-c) can take place, the last one under the condition:

$$\varepsilon > \frac{2\alpha^2}{2 - \lambda z} \frac{4 \ln g_1 - 3 \ln g_0 - \ln g_2}{2 \ln g_1 - \ln g_0 - \ln g_2}.$$

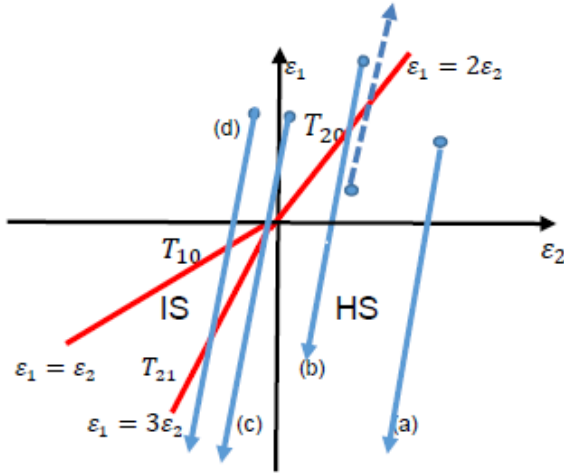


Figure 1. Phase diagram in the plane  $\varepsilon_2 - \varepsilon_1$ , showing high spin (HS), intermediate spin (IS) and low spin (LS) phases, the equilibrium curves (red lines) and the possible positions of the ground state (blue points). Arrows (a)-(d) indicate the evolution of phase points as temperature increases at constant pressure for  $g_0 = 1$ ;  $g_1 = 9$ ;  $g_2 = 15$  and different positions of the ground state (small circles). The broken arrow qualitatively represent the evolution of the phase point as pressure increases at constant temperature.

When long-range interactions are present ( $4 > \lambda z > 2$ ), the LS ground state is in the second quadrant and temperature-induced two-step transitions take place (isobar-d). This condition is sufficient but not necessary: two-step transitions can occur also in the absence of long range interactions (isobar-c).

Within this model, the occurrence of a IS homogeneous phase and two-steps transitions relies on the existence of excited states  $t_{2g}^5 e_g^1$  with total spin  $S = 1$  in an isolated complex [SA]. For an infinite system of coupled complexes, the phase with all Fe(II) atoms in  $S = 1$  states will never represent the ground state, but it could be stabilized at non-zero temperature by the combined effect of interactions and entropy (it has larger degeneracy than the LS state). As shown in the diagram, this phase has the lower free energy for  $0 > \varepsilon_2 > \varepsilon_1 > 3\varepsilon_2$ . If the  $S = 1$  local states are not considered, only HS and LS phases arise, separated by the straight line  $\varphi_2 = 0$ .

When only  $n_i = 0, 2$  values are admitted, the effective electron Hamiltonian 10 can be reduced to an Ising model in the pseudo spin variables  $\sigma_i = n_i - 1$ , with a temperature dependent external field  $h(T)$ . The ferromagnetic Ising model with short range interactions has a first order phase transition between spin up and a spin down phases only for  $h = 0$  and  $T < T_c$  with  $T_c$  the Curie temperature. These two conditions set limits to the existence of the LS-HS transition and define its temperature  $T_{20}$  in terms of model parameters. However, the jump of the order parameter  $\Delta n(T_{20}) < 2$  is different from the  $\Delta n \approx 2$  observed in SCO systems. On the other hand, for the Ising model with near-neighbors interaction, the IS phase could only result from alternating spin order induced by antiferromagnetic coupling and could not coexist in the same material with the HS phase, which needs ferromagnetic coupling. So, Ising models with short range interactions do not describe the basic phenomenology of SCO. In reference [14] an Ising model with short and long range interactions, the latter treated in mean field

approximation, has been considered to discuss two-steps transitions in one-dimensional SCO chains.

The HS $\leftrightarrow$ LS, HS $\leftrightarrow$ IS, IS $\leftrightarrow$ LS transition temperatures  $T_{20}$ ,  $T_{21}$ ,  $T_{10}$  are respectively:

$$\begin{aligned} kT_{20} \ln \left( \frac{g_2}{g_0} \right)^{1/2} &= \varepsilon - \frac{4\alpha^2}{2 - \lambda z} \\ kT_{21} \ln \left( \frac{g_2}{g_1} \right)^{1/2} &= \varepsilon - \frac{6\alpha^2}{2 - \lambda z}, \\ kT_{10} \ln \left( \frac{g_1}{g_0} \right)^{1/2} &= \varepsilon - \frac{42\alpha^2}{2 - \lambda z}. \end{aligned} \quad (15)$$

For  $\varepsilon = 1600 \text{ cm}^{-1}$ ,  $\hbar\omega = 180 \text{ cm}^{-1}$  and taking  $\alpha = 1$ ;  $\lambda = 0.25$ ;  $z = 6$  a reasonable HS $\leftrightarrow$ LS transition temperature  $T_{20} = 170 \text{ K}$  is obtained from 15.

As previously stated, all energy parameters have been expressed in units of the local breathing mode energy  $\hbar\omega$ . In ordinary units one has:

$$\varepsilon_2 = \frac{2\alpha^2 \hbar\omega}{2 - \lambda z} - \frac{kT}{2} \ln \left( \frac{g_1^2}{g_2 g_0} \right).$$

In the framework of this simple model  $\alpha, \lambda, \omega, \varepsilon$  are intuitively expected to increase with pressure. Then, parameters  $\varepsilon_1$  and  $\varepsilon_2$  are also growing functions of pressure. On the other hand, combining 13 with general thermodynamics:

$$\left( \frac{\partial \varepsilon_1}{\partial p} \right)_T n - \left( \frac{\partial \varepsilon_2}{\partial p} \right)_T n^2 = \left( \frac{\partial f}{\partial p} \right)_T \geq 0.$$

Consequently, for  $n = 1, 2$  as pressure increases at constant temperature  $\varepsilon_1$  grows faster than  $\varepsilon_2$  and the system always approaches lower spin phases. The qualitative evolution of the phase point as been represented in the phase diagram with a discontinuous arrow. Determining the exact equation of these isotherms requires the specification of the (unknown in this description) pressure dependence of parameters  $\varepsilon_1$  and  $\varepsilon_2$ . Increasing pressure increases transition temperatures. Pressure induced transitions HS $\leftrightarrow$ LS could take place for systems with a HS ground state, which do not experience temperature induced transitions, as experimental evidence shows [1] and the phase diagram illustrates. Dimensionality enters the phase diagram through the number of near neighbors  $z$ . A larger  $z$  is equivalent to a stronger coupling between neighboring breathing modes and favors HS states. Consider, for example, layered materials obtained by assembling planes of coupled octahedral complexes separated by organic linkers. As inter-plane coupling is weak, the ground state moves to the LS region  $\varepsilon > (4\alpha^2 \hbar\omega)/(2 - \lambda z)$  and the quasi 2D systems ( $z = 4$ ) can show SCO even when their 3D counterpart ( $z = 6$  without the organic linker) is always in the HS state. This behavior has been observed in layered Fe nitroprussides [15]. If there is SCO in the 3D system, it is expected to take place at a higher temperature in the layered version.

The phase diagram previously presented could be modified by considering non-homogeneous phases, which means



considering the contribution of the last term in expression 11 for the free energy functional. According to 11 and 12, one has  $\varepsilon_2(\vec{q}) < \varepsilon_2 < 0$  for  $\lambda z > 2$ . In this case, spatial fluctuations always increase the free energy and disappear from the minimum configuration. This means that for phase points in the third and fourth quadrants local order is preserved without spatial fluctuations across the crystal.

On the contrary, in the weak coupling case, when  $\varepsilon_2 > 0$  so that  $\varepsilon_2(\vec{q}) > 0$ , at least for small  $q$ , long range fluctuations lower the free energy and could destroy the homogeneous phase. Fortunately, the free energy functional with fluctuations included has a lower bound given by:

$$\begin{aligned}\varphi &= \varphi_n - \sum_{\vec{q} \neq 0} \varepsilon_2(\vec{q}) |\tilde{n}(\vec{q})|^2 > \varphi_n - \varepsilon_2 \sum_{\vec{q} \neq 0} |\tilde{n}(\vec{q})|^2 \\ &= \varphi_n - \varepsilon_2 \left( \frac{1}{N} \sum_i n_i^2 - n^2 \right) \geq \varepsilon_1 n - 4\varepsilon_2.\end{aligned}$$

It follows that:

$$\min(\varepsilon_1 n - 4\varepsilon_2) \leq \min(\varphi) \leq \min(\varphi_n). \quad (16)$$

In the fourth quadrant of the phase diagram ( $\varepsilon_1 < 0$ ;  $\varepsilon_2 > 0$ ) the only possible minimum of the free energy functional consistent with 16 is obtained for  $n = 2$  and  $\varepsilon = \varepsilon_2$ , which corresponds to a stable high temperature HS phase for:

$$T = \frac{2\varepsilon}{k(4 \ln g_1 - 3 \ln g_0 - \ln g_2)}$$

As temperature decreases below this value and the phase point moves to the first quadrant ( $\varepsilon_1 > 0$ ;  $\varepsilon_2 > 0$ ), the minimum of the free energy functional can be reached for average spin values different from those corresponding to homogeneous phases with  $n = 0, 2$ , as shown in figure 2.

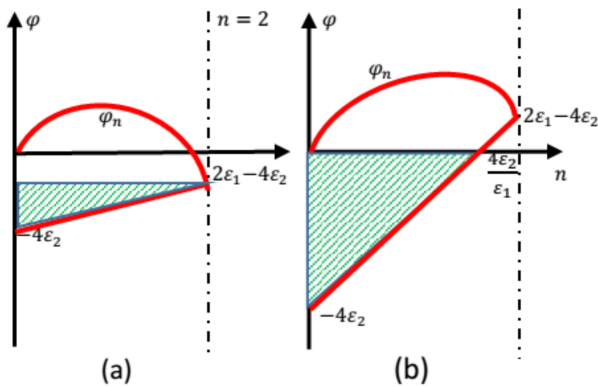


Figure 2. In the first quadrant of the phase diagram ( $\varepsilon_1 > 0$ ;  $\varepsilon_2 > 0$ ), the minimum of the Landau free energy  $\varphi$  lies in the shadowed region between the straight line  $\varepsilon_1 n - 4\varepsilon_2$  and the curve  $\varphi_n = \varepsilon_1 n - \varepsilon_2 n^2$  (both in red) (a)  $T > T_{20}$ ; (b)  $T < T_{20}$

In the HS phase (figure 2a), configurations with different average spin and nearly equal free energy are unstable, which combined with large relaxation times, needed to change the spin state of a macroscopic fraction of the ions in the

sample, can lead to hysteresis. Notice that for the system in the state  $n=0$  there is a free energy barrier to transit to the equilibrium state  $n = 2$ . At temperatures lower than the mean field transition temperature  $T_{20}$  (figure 2b) the minimum free energy can be reached for any average spin value  $n \leq (4\varepsilon_2)/\varepsilon_1$  which, again combined with large relaxation times, can also lead to hysteresis and incomplete transitions at very low temperatures. Notice now for the system with  $n = 2$  there is a free energy barrier to transit to the equilibrium value  $n = 0$ . The description of these phenomena requires full consideration of spin fluctuations and can be approached with the aid of Monte Carlo simulations.

The model presented in this paper could also be applied to discuss SCO in nanoparticles [16]. However, it must be emphasized that the minimum of the free energy functional corresponds to the exact free energy per site only in the thermodynamic limit. For small samples, fluctuations with respect to that minimum and boundary conditions play a very important role and should be considered. Model extensions to evaluate lattice entropy changes during transitions, an important experimental fingerprint of SCO not considered here, are also possible. Local fields describing the interaction between spin centers in binuclear SCO compounds and other effects of the chemical environment can be also incorporated to the model.

#### IV. CONCLUSIONS

A simple model of  $e_g$  electrons at octahedral sites interacting with local breathing modes coupled to its near neighbors, accounts for the basic phenomenology of spin crossover in molecular crystals formed with Fe (II) complexes. The effective electron-electron interaction can be short or long ranged, attractive or repulsive, depending on inter-site coupling and site connectivity. An exact analytic expression for the free energy functional has been derived. A diagram has been obtained for homogeneous phases and the transition temperatures have been calculated in terms of model parameters. Two-step transitions are possible for systems with both, short range and long range interactions. Instability with respect to spatial fluctuations appears near the HS↔LS transition, which combined with large relaxation times can lead to hysteresis and incomplete transitions. .

#### SUPPLEMENTARY INFORMATION

Details of long demonstrations contained in supplements SA, SB and SC are freely available on-line.

#### ACKNOWLEDGEMENTS

CRC and YMP acknowledge the support of CONACyT through scholarships for a sabbatical year and MSc study program respectively. This study was partially supported by the CONACyT projects 2013-05-231461 and CB-2014-01-235840.

## REFERENCES

- [1] P. Gütlich and H. A. Goodwin, Eds. Spin crossover in transition metal compounds I, II, III. Springer series "Topics in current Chemistry" Vol. 233-235 (2004).
- [2] M.A. Halcrow. Spin-crossover materials: properties and applications (John Wiley and Sons, 2013).
- [3] P. Gütlich, A.B. Gaspar and Y. García, *Bellstein J. Org. Chem.* **9**, 342 (2013)
- [4] C. Kohler, R.Jakobi, E.Meissner, L.Wiehl, H.Spiering, P.Gütlich, *J. of Phys. Chem. Solids* **51**, 239 (1990).
- [5] C. M. Jureschi, J. Linares, A. Rotaru, M. H. Ritti, M. Parlier, M. M. Dîrtu, M. Wolff, and Y. Garcia, *Sensors*, **15**, 2388 (2015).
- [6] D. Chernyshov, H.-B. Burgi, M. Hostettler and K.W. Tornroos, *Phys. Rev. B*, **70**, 094116 (2004).
- [7] J. Wajnsflasz and R. Pick, *J. Phys. Colloq.*, **32**, 1 (1971).
- [8] A. I. Nesterov, Y.S. Orlov, S. G. Ovchinnikov and S. V. Nikolaev, *Phys. Rev. B*, **96**, 134103 (2017).
- [9] A. Palii, S. Ostrovsky, O. Reu, B. Tsukerblat, S. Decurtins, Shi-Xia Liu, and S. Klokishner, *The Journal of Chemical Physics*, **143**, 084502 (2015).
- [10] T. Kambara, *J. Chem. Phys.* **70**, 4199 (1979).
- [11] T. Kambara, *J. Chem. Phys.* **74**, 4557 (1981).
- [12] A. Palii, S. Ostrovsky, O. Reu, B. Tsukerblat, S. Decurtins, Shi-Xia Liu, and S. I. Klokishner. *J. Phys. Chem. C* **120**, 14444 (2016).
- [13] S. Klokishner, J. Linares, and F. Varret, *Chem. Phys.* **255**, 317 (2000).
- [14] D. Chiruta, J. Linares, P. R. Dahoo and M. Dimian, *J. Appl. Phys.* **112**, 074906 (2012).
- [15] V. Niel, J. M. Martínez-Agudo, M. C. Muñoz and J. A. Real, *Inorg. Chem.* **40**, 3838 (2001).
- [16] T. Kawamoto and S. Abe, *Chem. Commun.* **31**, 3933 (2005).

---

This work is licensed under the Creative Commons Attribution-NonCommercial 4.0 International (CC BY-NC 4.0, <http://creativecommons.org/licenses/by-nc/4.0>) license.

